n-type doping in Cd_2SnO_4: A study by EELS and photoemission

Y. Dou and R. G. Egdell*
Inorganic Chemistry Laboratory, South Parks Road, Oxford OX1 3QR, United Kingdom
(Received 20 November 1995; revised manuscript received 19 January 1996)

The influence of n-type doping on the electronic structure of Cd_2SnO_4 has been studied by electron-energy-loss spectroscopy (EELS) and UV photoemission spectroscopy (UPS). In substitution on Cd sites or Sb substitution in Sn sites leads to the the appearance of well-defined plasmon loss peaks in EELS, with a maximum plasmon energy of just below 0.6 eV in Sb-doped material. A weak conduction-band feature is observed in UPS, the width of which is of the order expected from a simple free-electron model. [S0163-1829(96)00720-5]

I. INTRODUCTION

The post transition-metal oxides In_2O_3 and SnO_2 are of significant technological interest because they are wide-gap materials [E_{gap}=3.62 eV (Ref. 1) for SnO_2; E_{gap}=3.75 eV (Ref. 2) for In_2O_3] which when n-type doped combine the properties of optical transparency in the visible region with high electrical conductivity and high reflectivity in the infrared.[3] Doping can be achieved either by oxygen deficiency or by chemical substitution of Sn for In or of Sb for Sn. The range of high infrared reflectivity is governed by the carrier concentration, which in turn determines the energy of the conduction-electron plasmon. Maximum plasmon energies of 0.59 (Ref. 4) and 0.63 eV (Ref. 5) have been observed in ceramic samples of Sb-doped SnO_2 and Sn doped In_2O_3, respectively. The plasmon energies which can be achieved in CdO doped by analogous In substitution exceed those for In_2O_3 and SnO_2 [the maximum value that we have observed in a ceramic is 0.72 eV (Ref. 6)], but CdO is of little use as a transparent conducting material, owing to the much smaller band gap of the host oxide [E_{gap}=0.55 eV for CdO at 300 K (Ref. 7)]. The ternary oxides $CdIn_2O_4$ (E_{gap}=2.23 eV) and Cd_2SnO_4 (E_{gap}=2.06 eV) have bigger band gaps[8] than CdO itself and the visible absorption edge moves to much higher energy with n-type doping, due to the exceptionally large Moss-Burnstein shift associated with the low carrier effective mass.[9–11] These oxides, therefore, stand alongside In_2O_3 and SnO_2 as potential transparent conducting materials. n-type doping of Cd_2SnO_4 can be produced by subjecting thin-film material to reducing conditions, which presumably produce donor oxygen vacancies. However, by analogy with the binary systems discussed above, it is to be expected that substitution of In onto Cd sites or Sb onto Sn sites will produce n-type doping. There have been previous studies of Sb doped Cd_2SnO_4 by NMR (Refs. 12–14) and conductivity[15] measurements, but as far as we know, there has been no previous systematic attempt to define the range of plasmon energies that can be achieved by substitutional doping.

In the present paper, we use electron-energy-loss spectroscopy to measure plasmon energies in In- and Sb-doped Cd_2SnO_4. In addition, photoemission measurements have been performed on these materials. These allow direct observation of the electrons introduced into the conduction band by doping. By considering the conduction bandwidth in relation to the plasmon energy in EELS, it is possible to explore the applicability of a free-electron model to the conduction electrons in these materials.

II. EXPERIMENT

Polycrystalline Cd_2SnO_4 and $Cd_2Sn_{1-x}Sb_xO_4$ ($0.00<x<0.05$) was prepared by firing well ground stoichiometric mixtures of CdO, SnO_2 and Sb_2O_3 at 1050 °C in air for 6 h. Material with up to five cation % Sb gave x-ray powder-diffraction patterns, which contained only reflections characteristic of the orthorhombic Cd_2SnO_4 structure,[16,17] but beyond this doping level, weak peaks characteristic of Sb_2O_3 were observed. $Cd_{2-x}In_xSnO_4$ ($0.00<x<0.04$) was prepared by firing $Cd_{1-x}In_xO$ and SnO_2, again at 1050 °C for 6 h. The $Cd_{1-x}In_xO$ was prepared by firing CdO and In_2O_3 at 850 °C for seven days. Phase pure material with the rocksalt structure of CdO was obtained for doping levels up to 2 at. %, beyond which level reflections, due to $CdIn_2O_4$ were observed in XRD. The $Cd_{2-x}In_xSnO_4$ prepared from phase pure $Cd_{1-x}In_xO$ was itself phase pure.

X-ray and ultraviolet photoelectron spectra (XPS and UPS) were measured in an ESCALAB 5 Mark I spectrometer equipped with a twin anode x-ray source and rare-gas discharge lamp. Samples were mounted on Pt stubs and held in position with Pt wires. Sample cleaning was achieved by annealing pellets for 2–3 h at around 400 °C (stub temperature) in the spectrometer preparation chamber (base pressure $<10^{-9}$ mbar), with the aid of a water cooled copper work coil coupled to a 400 KHz radiofrequency generator. Following transfer to the main chamber (base pressure 2×10^{-10} mbar) XPS were found to be completely free of signals due to carbon or other contamination. The O 1s core peak showed a single component, with no evidence of high-binding-energy shoulders, due to water or hydroxide contamination. Similarly, He(II) photoemission spectra contained no adsorbate-related peaks on the high-binding-energy side of the main O 2p valence band. The nominal analyzer resolution was set at 100 meV for He(I) photoemission measurements and at 400 meV for He(II) photoemission and XPS. Structure due to HeIβ and HeIγ satellite radiation was subtracted from spectra using an interactive stripping routine, which ensured optimal removal of satellite intensity

0163-1829/96/53(23)/15405(4)/$10.00 © 1996 The American Physical Society

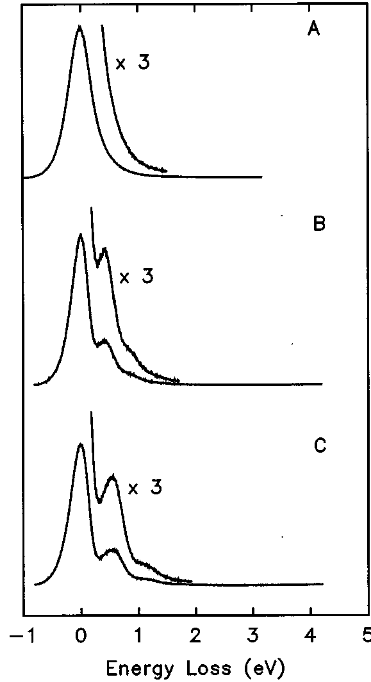

FIG. 1. EEL spectra of (A) nominally undoped Cd_2SnO_4, (B) $Cd_{1.96}In_{0.04}SnO_4$, and (C) $Cd_2Sn_{0.95}Sb_{0.05}O_4$ excited with a 200 eV electron beam. Note resolved plasmon loss peaks for the doped material.

subject to the constraint that there should be no negative dips in the stripped spectra. The position of the Fermi energy in the spectrometer was established from measurements on a sample of clean polycrystalline silver foil. Fermi levels of the degenerate conducting stannate samples should equalize with those of the silver and indeed a weak Fermi-Dirac-like onset was found for for the Cd_2SnO_4 samples at the same position as the silver onset. Binding energies are referred to this Fermi-Dirac onset. EEL spectra were measured in the same chamber using electrons from an electron gun forming part of a LEED optics. The analyzer resolution was set at the low value of 20 meV for these measurements, mainly to protect the channeltron from high incident electron fluxes in the elastic peak. The experimental resolution in EELS was however limited by the thermal spread of electrons from the electron gun.

III. RESULTS AND DISCUSSION

EEL spectra were measured for Sb-doped samples with $x=0.01$, 0.015, 0.02, 0.03, 0.04, and 0.05 and for In-doped samples with $x=0.01$, 0.02, 0.03, and 0.04. Typical EEL spectra in the energy-loss region close to the elastic peak are shown in Fig. 1, for undoped Cd_2SnO_4, $Cd_{1.96}In_{0.04}SnO_4$ and $Cd_2Sn_{0.95}Sb_{0.05}O_4$. For nominally undoped Cd_2SnO_4, there is no clearly defined plasmon loss, although the peak profile does show evidence of asymmetric broadening on the low-kinetic-energy side consistent with an unresolved loss feature at an energy of about 0.3 eV. However, for both doped samples, a resolved plasmon loss is observed, together with weaker losses at twice the principal loss energy arising from sequential inelastic scattering. The loss energies for the complete series of doped samples are summarized in Table I. It is clear that after a large increase with initial doping, the plasmon energy shows only small subsequent increases with doping.

TABLE I. Surface-plasmon energies and carrier concentrations in doped $Cd_2Sn_{1-x}Sb_xO_4$ and $Cd_{2-x}In_xSnO_4$.

x	Plasmon energy (eV)	Carrier concentration ($10^{18}/cm^3$)	Doping level ($10^{18}/cm^3$)	m^*/m_e
Sb doped				
0.010	0.445	71	40	0.098
0.015	0.465	78	59	0.103
0.020	0.510	119	79	0.126
0.030	0.550	168	119	0.152
0.040	0.580	212	158	0.174
0.050	0.595	239	198	0.186
In doped				
0.010	0.375	31	40	0.068
0.020	0.430	51	79	0.084
0.030	0.435	56	119	0.088
0.040	0.440	62	158	0.092

At the low beam energy of the present experiments, surface loss will predominate over bulk loss, i.e., the loss condition is determined by $\mathrm{Re}[\varepsilon(\omega)]=-1$ rather than $\mathrm{Re}[\varepsilon(\omega)]=0$.[18] The surface-plasmon frequency is given by

$$\omega_{sp}{}^2 = ne^2/[\varepsilon_0\{\varepsilon(\infty)+1\}m^*]$$

where n is the carrier concentration, $\varepsilon(\infty)$ is the background dielectric constant, and m^* is the conduction-electron effective mass at the Fermi energy. In the earlier work of Nozik *et al.*[9] and Miyata *et al.*,[10] $\varepsilon(\infty)$ was found to be 4.0 ± 0.1 and m^* was found to vary with carrier concentration. Empirically, we have found that the six values of m^* at differing carrier concentrations tabulated in this earlier work are best described in terms of a quadratic variation with Fermi wave vector k_F, i.e., m^* varies linearly with the $n^{2/3}$:

$$m^* = m_0^* + an^{2/3}$$

where $m_0^* = 0.02765m_e$ (m_e being the electron rest mass) and $a/m_e = 0.41\times10^{-14}$ cm^2. From this relationship it is possible to predict the variation in surface-plasmon energy with carrier concentration and thus to use the measured values of the loss energy to define the carrier concentration. The values obtained in this way (Table I) may be compared with the dopant concentration, which is fixed by the chemical concentrations in the reaction mixtures. From this analysis, it is clear that in Sb-doped material the actual carrier concentration always exceeds the nominal dopant level, typically by something of the order 40×10^{18} electrons/cm^3. Thus, it appears that Sb(V) is substitutionally incorporated onto Sn(IV) sites without compensation and that additional carriers arise from oxygen vacancy donor levels. The estimated plasmon energy of 0.3 eV for undoped material is consistent with a carrier concentration of about $12\times10^{18}/cm^3$, suggesting that oxygen vacancy donors are perhaps enhanced by Sb doping. In contrast to Sb doping, In doping gives carrier concentrations that are always lower than the dopant concentration.

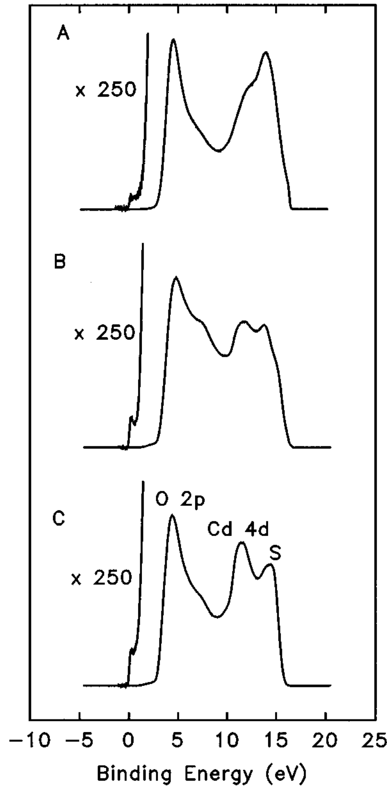

FIG. 2. He(I) photoemission spectra of (A) Cd_2SnO_4, (B) $Cd_{1.96}In_{0.04}SnO_4$, and (C) $Cd_2Sn_{0.95}Sb_{0.05}O_4$. Structure due to O $2p$ valence electrons, shallow core-level Cd $4d$ electrons, and secondary-electron emission (S) is labeled in (c). Binding energies are given relative to Fermi energy of a silver sample tub. Structure due to satellite radiation has been subtracted from the spectra.

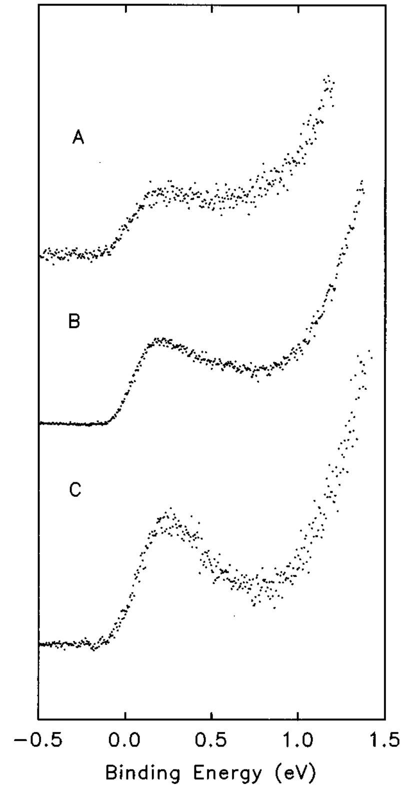

FIG. 3. Expanded He(I) photoemission spectra of (A) Cd_2SnO_4, (B) $Cd_{1.96}In_{0.04}SnO_4$, and (C) $Cd_2Sn_{0.95}Sb_{0.05}O_4$ in the region of the conduction band. Binding energies are given relative to Fermi energy of a silver sample stub. Structure due to satellite radiation has been subtracted from the spectra.

This could arise from compensation of In(III) substitution on Cd(II) sites by cation vacancies, although compensation of this sort does not pertain to CdO itself. However, a more likely explanation is that In(III) is distributed between Cd(II) and Sn(IV) sites. Whereas In(III) is a donor on the former, it is an acceptor on the latter. Thus, the availability of two different cation sites allows for substitutional incorporation of In with a carrier concentration lower than the nominal doping level.

He(I) photoemission spectra are shown in Fig. 2. The spectra are dominated by the O $2p$ valence band, the onset of which is about 3 eV below the Fermi energy. There is also a strong Cd $4d$ shallow core-level peak superimposed on the secondary-electron background. However, the major interest of the present paper centers on weak structure close to the Fermi energy, which arises from occupancy of the conduction band. The conduction-band feature is weaker in nominally undoped Cd_2SnO_4 than for either of the doped samples. This is consistent with the EELS measurements, which suggest a low but not vanishing carrier concentration in Cd_2SnO_4. The conduction band derives from Sn and Cd $5s$ atomic orbitals, both of which have very low one-electron ionization cross sections relative to the cross section for O $2p$ states at $h\nu=21.2$ eV [σ(Cd $5s$)=3.25×10^{-2} MB; σ(Sn $5s$)=3.25×10^{-2} MB; σ(O $2p$)=2.67 MB (Ref. 19)]. Coupled with the relatively low doping levels, this accounts for the low intensity of the conduction-band structure. However, after prolonged spectral accumulation the conduction-band structure can be observed with adequate signal-to-noise ratio to allow definition of the shape and width of the band, as shown in Fig. 3. Here, it is clear that the band has a parabolic free-electron-like shape for both In- and Sb-doped samples. Although the variation of effective mass within the conduction-band precludes rigorous application of a free-electron model (which assumes strictly quadratic dispersion and constant m^*), it is nonetheless interesting to make a rough estimate of the the overall bandwidth E derived assuming a fixed m^* within the band. Such an analysis[20] has revealed essentially free-electron-like behavior for conduction electrons in doped SnO_2.

$$E=(h^2/4\pi^2m^*)(3\pi^2n)^{2/3}.$$

The estimated bandwidths are 0.62 eV for $Cd_{1.96}In_{0.04}SnO_4$ and 0.76 eV for $Cd_2Sn_{0.95}Sb_{0.05}O_4$. The experimental bandwidths are clearly of this order, although it is difficult to define the position of the lower edge of the conduction band.

In summary, we have studied the effects of In and Sb substitutional doping in Cd_2SnO_4 and have established that Sb acts as an efficient donor, which sponsors at least one carrier per dopant atom. By contrast, In doping is significantly compensated, possibly by substitution of In(III) onto Sn(IV) sites as well as the target Cd(II) sites.

*Author to whom correspondence should be addressed.

[1] V. T. Agekyan, Phys. Status Solidi, A **4**, 11 (1977).
[2] I. Hamberg, K. F. Bergren, L. Engstrom, C. G. Granquist, and B. E. Sernelius, Phys. Rev. B **30**, 3240 (1988).
[3] H. Köstlin, Festkörpeprobleme **XXII**, 229 (1982).
[4] R. G. Egdell, W. R. Flavell, and P. Tavener, J. Solid State Chem. **51**, 345 (1984).
[5] P. A. Cox, W. R. Flavell, and R. G. Egdell, J. Solid State Chem. **68**, 340 (1987).
[6] Y. Dou, T. Fishlock, and R. G. Egdell (unpublished).
[7] This gap is indirect. See, *Physics of II–VI and I–VII Compounds, Semimagnetic Semiconductors*, edited by O. Madelung, M. Schulz, and H. Weiss, Landolt-Börnstein, New Series, Group III, Vol. 17, Pt. b (Springer Verlag, Berlin, 1982).
[8] F. P. Koffyberg and F. A. Benko, Appl. Phys. Lett. **37**, 320 (1980).
[9] A. J. Nozik, Phys. Rev. B **6**, 453 (1972).
[10] N. Miyata, K. Miyake, K. Koga, and T. Fukushima, J. Electrochem. Soc. **127**, 918 (1980).
[11] M. S. Setty, J. Mater. Sci. Lett. **6**, 909 (1987).
[12] C. M. Cardile, R. H. Meinhold, and K. J. D. MacKenzie, J. Phys. Chem. Solids **48**, 881 (1987).
[13] K. J. D. MacKenzie, C. M. Cardile, and R. H. Meinhold, J. Phys. Chem. Solids **52**, 969 (1991).
[14] C. M. Cardile, Rev. Solid State Sci. **5**, 31 (1991).
[15] R. D. Shannon, J. L. Gillson, and R. J. Bouchard, J. Phys. Chem. Solids **38**, 877 (1977).
[16] A. J. Smith, Acta Crystallogr. **13**, 749 (1960).
[17] M. E. Bowden and C. M. Cardile, Powder Diffraction **5**, 36 (1990).
[18] If the loss intensity were dominated by a bulk loss process, the value of n/m^* deduced from the EEL data would be decreased by a factor $\sqrt{\varepsilon(\infty)/[\varepsilon(\infty)+1]}=\sqrt{(4/5)}=0.89$.
[19] J. J. Yeh and I. Lindau, At. Data Nucl. Data Tables **32**, 1 (1985).
[20] P. A. Cox, R. G. Egdell, C. Harding, A. F. Orchard, W. R. Patterson, and P. J. Tavener, Solid State Commun. **44**, 837 (1982).